

TETRACARBOXYPHENYLPORPHYRIN/TiO₂ COMPOSITE THIN FILMS AS SELECTIVE OPTICAL SENSORS FOR THE DETECTION OF VOLATILE ORGANIC COMPOUNDS (VOCs)

María G. Guillén^{*†}, Javier Roales[†], Belén Suárez[†], Tânia Lopes-Costa[†], José M. Pedrosa[†], Pedro Castellero^{††}, Ángel Barranco^{††}, Agustín R. González-Elipe^{††}

^{*}Corresponding author. E-mail: mariagonzalez88@gmail.com

[†]Departamento de Sistemas Físicos, Químicos y Naturales. Universidad Pablo de Olavide
Ctra. Utrera Km. 1, 41013 Sevilla, Spain

^{††}Instituto de Ciencia de Materiales de Sevilla, Universidad de Sevilla – CSIC
Américo Vespucio 49, 41092, Sevilla, Spain

Key words: Carboxyphenyl porphyrin, TiO₂ nanostructures, Thin films, Volatile Organic Compound, VOC, Optical gas sensing, Aggregation, Spectral imaging.

Summary: *A carboxylic acid substituted of a free-base porphyrin, 5,10,15,20-tetrakis(4-carboxyphenyl)-21H,23H-porphyrin, and 10 of its metal derivatives (para-TCPPs) have been used for optical gas sensing. For this purpose, microstructured columnar TiO₂ thin films prepared by GAPVD (glancing angle physical vapor deposition) have been used as host materials for the porphyrins. The composite porphyrin/TiO₂ films obtained from each of the 11 porphyrins have been exposed to 12 different volatile organic compounds (VOCs), and their respective gas-sensitive properties have been analyzed as a function of the spectral changes in their Soret band region in the presence of the analytes. The set of composite films has shown high selectivity to the analyzed volatile compounds. For each analyte, an innovative way of showing the different responses has been developed. By means of this procedure, an imagelike recognition pattern has been obtained, which allows an easy identification of every compound. In addition, the same substrate was used to host a Zn tetracarboxyphenyl porphyrin, whose carboxylic acid groups are in a meta position, Zn-(II)-5,10,15,20-tetra(3-carboxyphenyl)porphyrin (m-ZnTCPP). Owing to this change in the molecular structure, p-TCPP and m-TCPP molecules show different spatial geometry leading to a different binding of the porphyrins to the titania surface which, as a result, gives rise to a different degree of aggregation in the films. The sensing performance of the two systems has been assessed by analyzing the spectral changes in their UV-visible spectra under exposure to six volatile organic compounds. Although the TiO₂ matrix allow good sensing ability in both cases, the response of the m-ZnTCPP/TiO₂ composite has been found to be more intense than that of p-ZnTCPP, which has been attributed to the absence of aggregation between adjacent macrocycles. Moreover, the use of identification patterns also indicates that the meta derivative achieves a more selective recognition of the selected analytes.*

Detection of volatile organic compound (VOC) has been generally performed through the separation and identification of components using gas chromatography or similar techniques. These analyses, although accurate, are usually time-consuming and need a lot of post-processing.[1] Alternatively, electronic nose technologies have been used to detect several kinds of compounds by an array of different sensors, providing an instantaneous and holistic response to the particular gas.[2,3] These devices are generally based on metal–oxide semiconductors or conducting polymers.[4] They are appropriate for the discrimination of analytes of different chemical functionality, but not when these are within the same chemical class,[5] or when we try to detect metal-binding species.[6]

Porphyrins and other dyes have been widely used in the last decades for gas-sensitive purposes.[5,7–9] Their photochemical and photophysical properties make them ideal candidates for the optical detection of analytes. Thus, they can be precisely tuned by introducing substituents in their structure or coordinating metals to the porphyrin core.[8]

The presence of π – π interactions between porphyrins may cause aggregation when the molecules are deposited on solid substrates, which can result in broadening, shifting and splitting of the bands present in the uv-vis spectrum with respect to the porphyrin solution.[9] In the case of VOC detection, the interaction with this kind of compound may modify these interactions, resulting in modifications of the spectrum that can be used for sensing applications.[8] In the search of porphyrin-based sensors, a wide range of substrates can be used as solid support for these molecules, from glass (for example, in the Langmuir–Blodgett technique) [10–12] to silica gel.[5,6]

Originally developed by solar cell researchers, the use of carboxylic acid derivatized molecules and their ability to chemically bind to TiO_2 allows the easy fabrication of stable composite films.[13] However, TiO_2 films prepared for solar cell purposes are usually thick and very dispersive, and thus inappropriate for gas sensing when using UV-visible spectroscopy. Microstructured TiO_2 films prepared by glancing angle physical vapor deposition (GAPVD) provide the perfect substrate for these composite films, given their transparency, high porosity, low refractive index and controlled thickness.[14] Films prepared by this technique have been used previously for gas sensing purposes and have been found to enhance the sensing properties of the porphyrins due to their open pores that facilitate the access to incoming gaseous molecules.[15–17] Also, the conformation of the sensing molecule in these composites can be important, determining its chemical binding to the substrate, according to the spatial distribution of anchoring points, and may also influence its tendency to aggregate with other molecules. [18] A change in the position of the peripheral substituents in a porphyrin can lead to different aggregation status that may improve its sensing capabilities.[9]

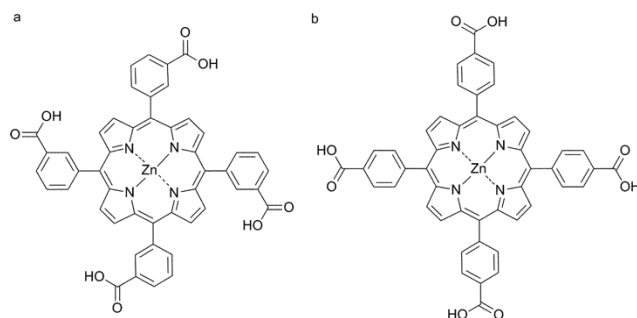


Figure 1 : Molecular structures of (a) Zn(II)-5,10,15,20-tetra(3-carboxyphenyl)porphyrin and (b) Zn(II)-5,10,15,20-tetra(4-carboxyphenyl) porphyrin.

Here we report the gas-sensitive properties of 5,10,15,20-tetrakis(4-carboxyphenyl)-21H,23H-porphyrin (*p*-TCPP) and 10 of its metal derivatives, using microstructured columnar TiO₂ thin films prepared by GAPVD as host materials.[17] The gas sensing capabilities of the composite *p*-TCPPs/TiO₂ thin films showed reversible, reproducible and selective responses to the analyzed VOCs, which have been represented as an imagelike recognition pattern. However, due to their chemical structure, *p*-TCPPs in these films can only anchor to the TiO₂ lying perpendicular with respect to the surface, which allow face to face interaction. It is known that the lack of aggregation enhances the sensing properties of porphyrins, allowing the gas molecules a better access to their coordination sites.[9] Therefore, the sensing system based on composite porphyrin/TiO₂ thin films may be improved by avoiding dye aggregation. On the other hand, *para* and *meta* substituted tetraphenyl porphyrins are known to exhibit a different molecular structure. [18,19] While the substituents in the *para* position of the phenyl groups are situated in the plane of the molecule, the *meta* substituents are placed in a perpendicular direction with respect to the porphyrin ring. Based on this different molecular architecture, it has been demonstrated that *para* tetracarboxyphenyl porphyrins only anchor to the TiO₂ by one or two of the four carboxylic groups lying perpendicular to the metal oxide surface, while the *meta* derivatives can bind its four COOH groups lying parallel to the TiO₂ surface.[18] Our hypothesis is that these different arrangements can lead to a different aggregation status of the porphyrin that may influence its sensing capabilities. For this reason, we studied composite films made of microstructured columnar TiO₂ and, respectively, Zn-(II)-5,10,15,20-tetra(3-carboxyphenyl)porphyrin (*m*-ZnTCPP, Fig. 1a) and Zn-(II)-5,10,15,20-tetra(4-carboxyphenyl)porphyrin (*p*-ZnTCPP, Fig. 1b) and their sensing properties regarding both the anchoring to the TiO₂ and the molecule aggregation are compared.[20] For this purpose, the chemical binding between the porphyrin and the TiO₂ has been confirmed through infrared spectroscopy. Besides, the influence of this binding on the aggregation and orientation of porphyrin molecules has been investigated. The optical responses of the two porphyrins to a total of 6 individual VOCs have been analyzed to test if the different peripheral substituent position plays an important role on the gas-sensing properties of these molecules.

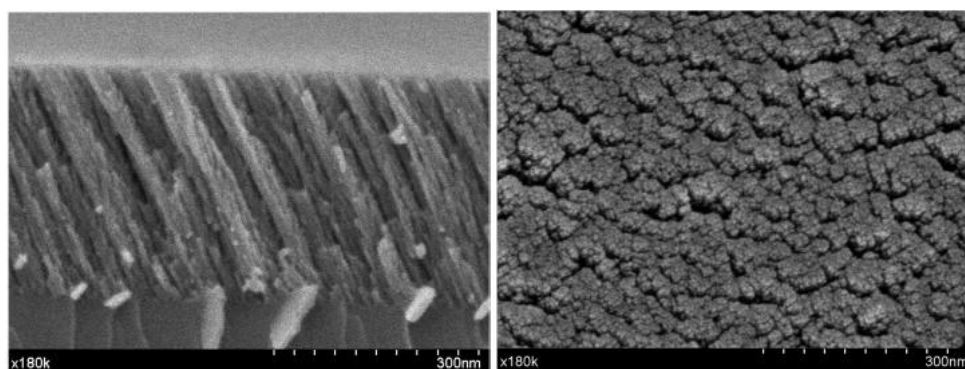


Figure 2 : (Left) Cross-section and (right) planar FESEM images of the columnar TiO₂ thin films prepared at an angle of deposition 70°.

Cross-section and normal FESEM images corresponding to TiO₂ thin films prepared by GAPVD at an angle of deposition of 70° are shown in Figure 2. The cross-section image shows the tilt angle of the columns and the thickness of the film. The angle formed by the columns and the substrate was found to be 60° with a film thickness of approximately 350

nm. The analysis of the images in Figure 2 reveals that the observed apertures correspond to mesopores (i.e., pores bigger than 2 nm) extending from the surface to the bottom of the film. This allows the accessibility of large molecules like porphyrins during the composite preparation and improves subsequent applications that would require a fast diffusion of gas molecules through the film structure.

Binding of the dye molecules to the TiO₂ films was carried out by immersing the films in a 10⁻⁴ M solution of the dye at room temperature (21 °C) for 1 h. The infiltrated films were rinsed, immersed in the same solvent to remove physisorbed dye and then dried.

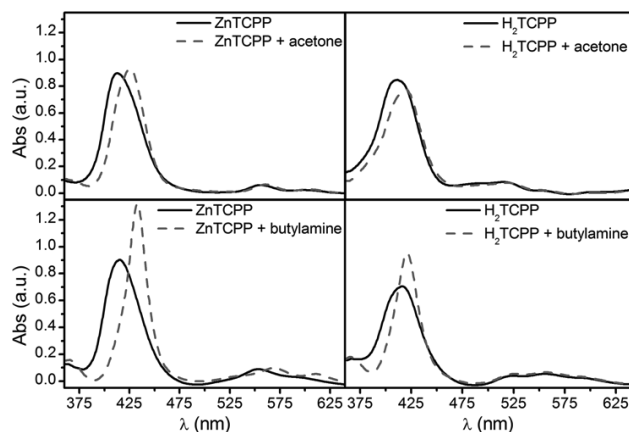


Figure 3 : Top: Before (solid line) and after (dashed line) exposure to acetone spectra of ZnTCPP/TiO₂ (left) and H₂TCPP/TiO₂ (right) composite films. Bottom: Before (solid line) and after (dashed line) exposure to butylamine spectra of ZnTCPP (left) and H₂TCPP (right) films.

Composite *p*-TCPP/TiO₂ films obtained from each one of the 11 porphyrins have been exposed to vapors of the following 12 different analytes: acetone, acetonitrile, chloroform, butylamine, dichloromethane, diethylether, dimethylformamide, ethanol, hexanethiol, hexylamine, methanol, and tetrahydrofuran. Figure 3 (top) shows the spectra of ZnTCPP and H₂TCPP composite films before and after their exposure to acetone. In the case of the ZnTCPP, the Soret band is red-shifted (13 nm) and increased after the exposure. The exposed H₂TCPP film spectrum shows less red shift (8.5 nm) and some decrease with respect to the pre-exposure spectrum. In Figure 5 (bottom), spectra of ZnTCPP and H₂TCPP films before and after exposure to butylamine are shown. In this case, the ZnTCPP Soret band is more red-shifted after the exposure than when exposed to acetone (17.5 nm), and the intensity of the absorbance is much more increased. However, the H₂TCPP spectrum shows a smaller shift (4.5 nm), and an intensity increase like in the case of the ZnTCPP derivative. In most cases, the spectral analysis showed significant differences of their respective spectral shifts and intensity changes when exposed to the different compounds. Through the recovery phase, samples returned to their original status. All samples showed good repeatability and reversibility. In addition, reproducibility of the response was good probably due to a complete saturation of the TiO₂ film by the infiltrated dye and the low variability in the film thickness.

A selective response can be obtained for each analyte through the analysis of the whole set of porphyrins, but owing to the large amount of collected information, a previous data processing stage is necessary in order to focus the attention on the spectral change.

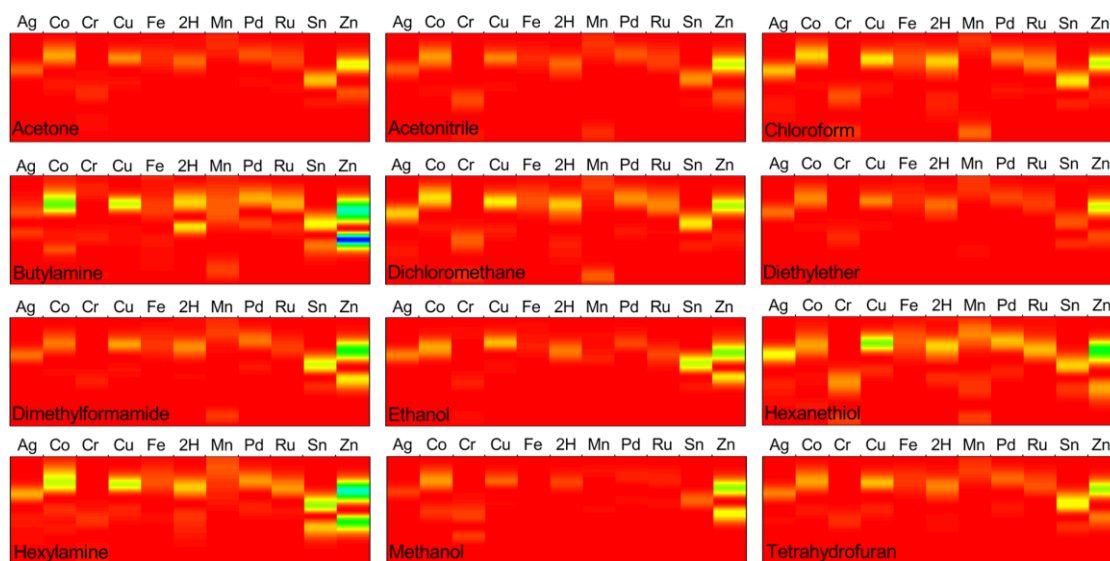


Figure 4: Identification patterns obtained for the different analytes. Color scale goes from red to blue, where red means no change between exposed and nonexposed spectra and blue is the highest change detected.

For this purpose, an innovative way of showing the response of all porphyrins to a certain analyte is shown in Figure 4. The resulting images possess spectral resolution and can be interpreted as recognition patterns for each analyte. Through these patterns, the shift and the change in absorbance intensity can be easily distinguished. By means of these images, like in the case of using bar codes, both the position and the intensity of the different bands give information about the compound to be identified. Each pattern consists of 11 columns corresponding to the 11 porphyrins used in this work. Every column shows the squared average difference of the post- and pre-exposure spectra in a color scale from red to blue, where red corresponds to no change between exposed and non-exposed spectra and blue is the highest change detected.

An image containing all these changes can be nowadays an ideal identification pattern given that cheap and versatile image-reading devices are available in the market. Additionally, the proposed approach is ready to access other spectral regimes such as the infrared, provided that new materials with sensing activity in that range are used, which enables this identification system to exploit optical sensing beyond the human-vision-based RGB colorimetric systems.

As can be seen in Figure 4, each analyte has a characteristic pattern that differs from the rest in one way or another, allowing the virtual identification of all analytes. Although some compounds show similarities to others, for example, acetone and acetonitrile or chloroform and dichloromethane have similar patterns, they are not identical. In particular, butylamine, hexylamine, hexanethiol, and dimethylformamide are the analytes that produce the highest values of change, especially when the exposed porphyrin is ZnTCPP, which is by far the most responsive.

Nevertheless, it was observed a blue-shift in the UV-visible spectra of the *p*-TCPP in these composite films (data not shown) which reveals that the dyes form aggregates when anchored to the TiO₂ film. Porphyrin aggregation could be detrimental for its gas sensing application due to a hindered access of the analytes to the porphyrin coordination sites.[9] However, it has been shown that such π - π interaction is not strong enough to avoid effective analyte binding probably due to the positive influence of the TiO₂ matrix whose chemical binding with the dye molecule prevents a closer position of their conjugated rings thus

avoiding a higher degree of aggregation. Anyway, a change in the position of the peripheral substituents in a porphyrin can lead to different aggregation status that may improve its sensing capabilities.[9]

For this reason, we studied composite films made of microstructured columnar TiO₂ and Zn-(II)-5,10,15,20-tetra(3-carboxyphenyl)porphyrin (*m*-ZnTCPP, Fig. 1a) and its sensing properties in order to compare them with the *p*-ZnTCPP ones regarding both the anchoring to the TiO₂ and the molecular aggregation.

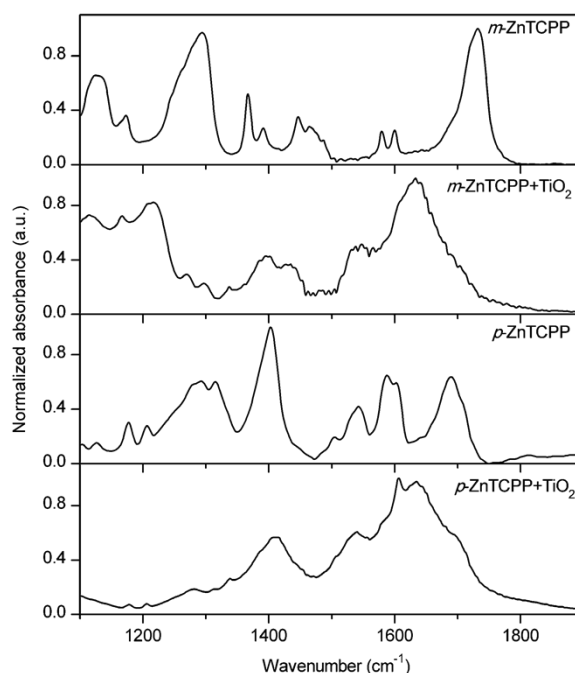


Figure 5 : Specular reflectance FT-IR spectra of *m*-ZnTCPP and *p*-ZnTCPP neat (by casting on silicon substrates) and bound to TiO₂.

We studied the binding of the carboxylic porphyrins to TiO₂ through specular reflectance FT-IR spectroscopy using a Jasco FT/IR-6200 spectrometer. Specular reflectance FT-IR spectra of *meta* and *para* porphyrins neat and bound to TiO₂ are shown in Fig. 5. In all cases, the existence of typical bands corresponding to the symmetric and asymmetric stretching modes of the pyrrole ring (ν (C–H), ν (C=C) and ν (C=N)) within the meso-tetraphenylporphyrin macrocycle was evident over the range 700–1500 cm⁻¹. [21] The binding interaction between the TCPP and the metal oxide surface is revealed by the comparison of changes in the region of the carbonyl group in the FT-IR spectra. Neat samples of *m*-ZnTCPP showed two strong bands at 1732 cm⁻¹ and 1294 cm⁻¹ which are characteristic of the ν (C=O) stretch and the ν (C–O) stretch of the carboxylic acid groups, respectively. In the case of *p*-ZnTCPP, where the –COOH groups are situated in the plane of the tetrapyrrole macrocycle, the extensive hydrogen bonding of the carboxylic acid groups resulted in a shift to lower frequency of the ν (C=O) stretch at 1690 cm⁻¹ and a shift to higher frequency of the ν (C–O) stretch at 1402 cm⁻¹. [22]

Upon binding of *m*-ZnTCPP to TiO₂, the ν (C=O) and ν (C–O) stretching modes disappeared completely, and new bands appeared in the 1385–1440 cm⁻¹ and 1530–1570 cm⁻¹ regions, corresponding to the symmetric and asymmetric ν (CO₂⁻) stretches, respectively. In

the case of *p*-ZnTCPP/TiO₂, the bands corresponding to the C=O and C–O stretching modes were still partially present with a slight broadening of the latter. In this case, the appearance of the band corresponding to the symmetric ν (CO₂⁻) stretch is not so evident due to overlapping with the remaining ν (C–O) stretch band. Moreover, the changes in the 1500–1750 cm⁻¹ region, where the asymmetric ν (CO₂⁻) stretch band was expected to appear, were hindered by the presence of a strong and broad band around 1630 cm⁻¹ corresponding to the free TiO₂ molecules of the columnar film.

Chemical binding of carboxylic acids to TiO₂ colloidal films has been associated with the disappearance of the bands corresponding to the ν (C=O) and ν (C–O) stretching modes, and the appearance of strong and broad bands at ~1400 cm⁻¹ and ~1550 cm⁻¹, characteristic of the symmetric and asymmetric ν (CO₂⁻) stretches respectively.[18] These spectral changes have been found to be compatible with chelating and/or bidentate binding modes of the carboxylate groups on the TiO₂ surface.[18, 23-26]

The IR spectrum of *m*-ZnTCPP/TiO₂ was consistent with the absence of free carboxylic acid groups, given that C=O and C–O stretching modes disappeared completely. This suggests a planar situation of the porphyrin macrocycle with respect to the titania surface in which all carboxyl groups are bound to the TiO₂. [18] However, in the case of *p*-ZnTCPP/TiO₂, the stretching modes corresponding to C=O and C–O disappeared only partially, indicating the presence of free carboxylic acid groups coexisting with carboxylate groups bound to TiO₂. As a result of this, and due to the planar structure of the para substituted porphyrins, it can be expected that they are bound only by one or two of its four carboxyl groups to the metal oxide surface, resulting in a perpendicular orientation of the molecule with respect to the surface that allows them to interact (face to face) with other molecules, causing aggregation.[18, 27]

UV-visible absorption spectra (data not shown) revealed that whereas the spectrum of *p*-ZnTCPP in the film featured a broadening and blue shift of the Soret band with respect to the solution spectrum indicating the H-aggregation of the dye,[18, 28, 29] only a slight broadening of the Soret band was shown in the case of *m*-ZnTCPP films indicating that the dye was predominantly in its monomeric form.

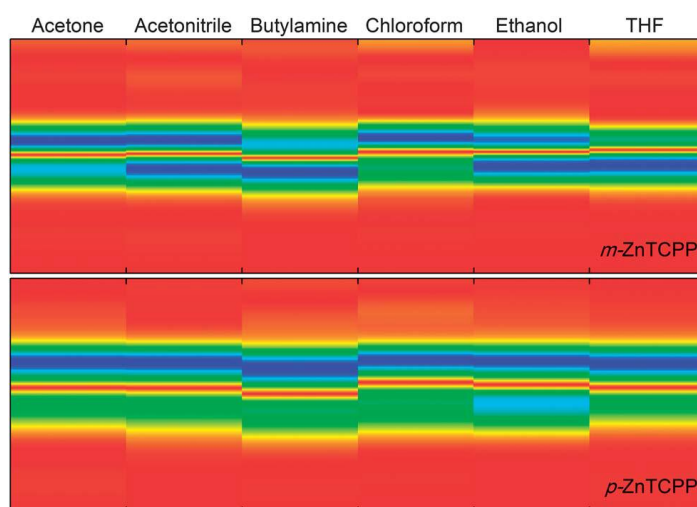


Figure 6 : Identification patterns obtained for acetone, acetonitrile, butylamine, chloroform, ethanol and tetrahydrofuran corresponding to *m*-ZnTCPP/TiO₂ and *p*-ZnTCPP. Color scale goes from red to blue, where red means no change between exposed and non-exposed spectra and blue is the highest change detected.

In order to study the differences in their sensing performance, spectral images of both porphyrins exposures to six different VOCs are shown in Figure 6. At a glance, it can be noticed that the patterns in *m*-ZnTCPP showed more variations among analytes than in the case of *p*-ZnTCPP. A more in-depth analysis of the images reveals that all bands corresponding to the different analytes in *m*-ZnTCPP showed appreciable differences among them, either in intensity or in position, which can be translated into a better selectivity of the system. On the contrary, *p*-ZnTCPP identification patterns were clearly more uniform. In particular, the patterns corresponding to acetone, acetonitrile and tetrahydrofuran are almost identical. In this case, the discrimination of these analytes using only the spectral information provided by the *para* substituted porphyrin would be difficult.

Regarding the comparison of our two systems, *m*-ZnTCPP kinetics was twice as fast as *p*-ZnTCPP. This difference in the speed of response and in the identification patterns analysis, show that *m*-ZnTCPP/TiO₂ films exhibited better gas-sensing properties than those based on *p*-ZnTCPP. This confirms that the positioning of the carboxylic acids in *meta* position in the porphyrins studied here improves considerably the sensing capabilities of the porphyrin/TiO₂ system. Therefore, our hypothesis that a change in the position of the peripheral substituents in a porphyrin can lead to different aggregation status that may improve its sensing performance, either in terms of response magnitude or kinetics can be validated.

9 CONCLUSIONS

Composite porphyrin/TiO₂ films based on microstructured columnar TiO₂ as host material and either *p*-TCPPs or *m*-ZnTCPP as sensing molecules have been prepared. Specular reflectance FT-IR has confirmed that the chemical binding of the two porphyrins to the TiO₂ is different depending on the corresponding position of the carboxylic acid groups. In particular, the dye molecules with the COOH groups in *meta* position were bound by their four carboxylic groups, whereas two or three of these groups remained unanchored in the *para* derivative. When hosted in the film, *p*-ZnTCPP featured a broadening and blue shift of the Soret band with respect to the solution spectrum, which indicated that the dye molecules were arranged mostly as H-aggregates. In contrast, the spectrum of *m*-ZnTCPP remained in its monomeric form, which has been attributed to the planar anchoring by the four carboxylic groups to the titania matrix that would prevent porphyrin aggregation.

The gas-sensitive properties of the composite films have been studied, showing a good selectivity to the analyzed volatile compounds. In the case of *p*-TCPPs, an image-like identification pattern based on spectral imaging has been obtained for each analyte, which facilitates the straightforward recognition of every compound.

In order to compare their response to several analytes, their corresponding image-like identification patterns based on spectral images were obtained for both *p*-TCPP and *m*-TCPP. They clearly show that the *meta* derivative offers a more selective response to the different analytes, paving the way for the preparation of multisensor arrays based on metal derivatives of *m*-TCPP with enhanced selectivity towards isolated and mixed analytes.

Overall, the *m*-ZnTCPP/TiO₂ films exhibited better gas-sensing properties than those based on *p*-ZnTCPP as a consequence of the different position of the peripheral carboxylic groups, whose specific anchoring to the titania surface leads to a different aggregation state in the solid film.

REFERENCES

- [1] H.T. Nagle, S.S. Schiffman, R. Gutierrez-Osuna, *IEEE*
- [2] J.W. Gardner, B.N. Bartlett, *Electronic Noses: Principles and Applications*, Oxford University Press, New York, 1999.
- [3] F. Röck, N. Barsan, U. Weimar, *Chem. Rev.*, **108**, 705–725, 2008.
- [4] K.J. Albert, N.S. Lewis, C.L. Schauer, G.A. Sotzing, S.E. Stitzel, T.P. Vaid, D.R. Walt, *Chem. Rev.*, **100**, 2595–2626, 2000.
- [5] N.A. Rakow, A. Sen, M.C. Janzen, J.B. Ponder, K.S. Suslick, *Angew. Chem., Int. Ed.*, **44**, 4528–4532, 2005.
- [6] N.A. Rakow and K.S. Suslick, *Nature*, **406**, 710–713, 2000.
- [7] K.S. Suslick, D.P. Bailey, C.K. Ingison, M. Janzen, M.E. Kosal, W.B. McNamara III, N.A. Rakow, A. Sen, J.J. Weaver, J.B. Wilson, C. Zhang and S. Nakagaki, *Quim. Nova*, **30**, 677–681, 2007.
- [8] C. Di Natale, R. Paolesse, A. D'Amico, C. Dinatale, A. Damico, *Sens. Actuators, B*, **21**, 238–246, 2007.
- [9] J.M. Pedrosa, C.M. Dooling, T.H. Richardson, R.K. Hyde, C.A. Hunter, M.T. Martín, L. Camacho, *Langmuir*, **18**, 7594–7601, 2002.
- [10] J.M. Pedrosa, C.M. Dooling, T.H. Richardson, R.K. Hyde, C.A. Hunter, M.T. Martín, L. Camacho, *J. Mater. Chem.* **12**, 2659–2664, 2002.
- [11] G. De Miguel, M.T. Martín-Romero, J.M. Pedrosa, E. Muñoz, M. Pérez-Morales, T.H. Richardson, L. Camacho, *J. Mater. Chem.*, **17**, 2914–2920, 2007.
- [12] J. Roales, J.M. Pedrosa, P. Castellero, M. Cano, T.H. Richardson, *Thin Solid Films*, **519**, 2025–2030, 2011.
- [13] W.M. Campbell, A.K. Burrell, D.L. Officer, K.W. Jolley, *Coord. Chem. Rev.*, **248**, 1363–1379, 2004.
- [14] J.R. Sánchez-Valencia, A. Borrás, A. Barranco, V.J. Rico, J.P. Espinós, A. R. González-Elipe, *Langmuir*, **24**, 9460–9469, 2008.
- [15] P. Castellero, J.R. Sánchez-Valencia, M. Cano, J.M. Pedrosa, J. Roales, A. Barranco, A.R. González-Elipe, *ACS Appl. Mater. Interfaces*, **2**, 712–721, 2010.
- [16] M. Cano, P. Castellero, J. Roales, J.M. Pedrosa, S. Brittle, T. Richardson, A. R. González-Elipe and A. Barranco, *Sens. Actuators, B*, **150**, 764–769, 2010.
- [17] J. Roales, J.M. Pedrosa, P. Castellero, M. Cano, T.H. Richardson, A. Barranco, A.R. González-Elipe, *ACS Appl. Mater. Interfaces*, **4**, 5147–5154, 2012.
- [18] J. Rochford, D. Chu, A. Hagfeldt, E. Galoppini, *J. Am. Chem. Soc.*, **129**, 4655–4665, 2007.
- [19] B.R. Takulapalli, G.M. Laws, P.a. Liddell, J. Andréasson, Z. Erno, D. Gust, T.J. Thornton, *J. Am. Chem. Soc.*, **130**, 2226–2233, 2008.
- [20] J. Roales, J.M. Pedrosa, M. Cano, M.G. Guillén, T. Lopes-Costa, P. Castellero, A. Barranco, A.R. González-Elipe, *RSC Adv.*, **4**, 1974–1981, 2014.
- [21] B. Long, K. Nikitin and D. Fitzmaurice, *J. Am. Chem. Soc.*, **125**, 5152–5160, 2003.
- [22] E. Galoppini, J. Rochford, H. Chen, G. Saraf, Y. Lu, A. Hagfeldt, G. Boschloo, *J. Phys. Chem. B*, **110**, 16139–16161, 2006.
- [23] G. Deacon, R. Phillips, *Coord. Chem. Rev.*, **33**, 227–250, 1980.
- [24] K.S. Finnie, J.R. Bartlett, J.L. Woolfrey, *Langmuir*, **14**, 2741–2749, 1998.
- [25] A. Vittadini, A. Selloni, F.P. Rotzinger, M. Grätzel, *J. Phys. Chem. B*, **104**, 1300–1306, 2000.
- [26] M.K. Nazeeruddin, R. Humphry-Baker, P. Liska, M. Grätzel, *J. Phys. Chem. B*, **107**,

María G. Guillén, Javier Roales, Belén Suárez, Tânia Lopes-Costa, José M. Pedrosa, Pedro Castellero, Ángel Barranco, Agustín R. González-Elípe

8981–8987, 2003.

[27] J. Rochford and E. Galoppini, *Langmuir*, **24**, 5366–5374, 2008.

[28] N. Aratani, A. Osuka, H.S. Cho, D. Kim, *J. Photochem. Photobiol., C*, **3**, 25–52, 2002.

[29] M.-S. Choi, *Tetrahedron Lett.*, **49**, 7050–7053, 2008.